Mg_2SiO_4-$MgAl_2O_4$ directionally solidified eutectics: Hardness dependence modelled through an array of screw dislocations

Bibi Malmal Moshtaghioun[a],[*], Diego Gomez-Garcia[b], Jose I. Peña[a]

[a] Instituto de Ciencia de Materiales de Aragón, CSIC-Universidad de Zaragoza, 50018 Zaragoza, Spain
[b] Departamento de Física de la Materia Condensada, CSIC-Universidad de Sevilla, P. O. 1065, 41080 Sevilla, Spain

ABSTRACT

Mg_2SiO_4-$MgAl_2O_4$ eutectic ceramics have been fabricated by means of the laser floating zone (LFZ) technique. The microstructure has revealed as an unusual one at lower growth rate, composed of broken lamellae of $MgAl_2O_4$ distributed randomly along one matrix, composed of Mg_2SiO_4. At higher growth rates, a cell structure with intra-cell lamella structure is dominant. Contrary to most eutectic systems, hardness is not dependent upon the inter-spacing, but it does depend on one characteristic length of lamellae: their perimeter. One simple model based upon the dislocation is proposed, which successfully accounts for such extraordinary hardness law. Accordingly, Mg_2SiO_4-$MgAl_2O_4$ eutectic ceramics fabricated at 50 mm/h growth rate with the smallest $MgAl_2O_4$ lamella perimeter favorably showed more elevated hardness (13.4 GPa from Vickers indentation and 15.3 GPa from nanoindentation) and strength (~430 MPa) than those found in the monolithic Mg_2SiO_4 matrix.

1. Introduction

There is a growing demand of forsterite (Mg_2SiO_4) ceramics to be used in a myriad of electronic applications due to its low dielectric constant and loss tangent. Moreover, it is one of the well-known bio-ceramics thanks to its reasonable biocompatibility and better mechanical properties when comparing with hydroxyapatite. Furthermore, forsterite is a classical refractory ceramic that is commonly used owing to its chemical stability and excellent insulation properties even at high temperatures. However, the main drawback of this ceramic is the fabrication of dense forsterite bodies and its negative influence on mechanical properties [1–9]. It can be found in the literature that by conventional sintering techniques like pressures-less sintering, forsterite possesses a low relative density around 90–93% with low hardness of 7 GPa and excessive grain growth is observed. Regarding fracture toughness, it depends on the experimental method: a value as low as 2.4 MPa m$^{1/2}$ is obtained making use of notched beams and bending tests while it goes up to 5 MPa m$^{1/2}$ by means of the indentation fracture toughness technique. Several authors doubt about this improvement and claim that it is a mere artifact because of remaining porosity [2–6].

A substantial purpose for the development of forsterite ceramics was recently demonstrated to improve sinterability, physicomechanical properties, strength and mechanical performance. To reach fully dense forsterite, some new sintering techniques like two step sintering and spark plasma sintering (SPS) also were tried and the improvement in sinterability to relative density of 98.5–99% and hardness values up to 10.8 GPa with indentation fracture toughness of ~4 MPa m$^{1/2}$ attained [7–9]. Another alternative to overcome with these limitations of forsterite was through addition of second phase and the most preferred one that can be sintered in an oxidizing atmosphere and withstand high mechanical strength at elevated temperatures, high chemical inertness, and good thermal shock resistance was magnesium aluminate spinel ($MgAl_2O_4$) [10–13]. Previous studies confirmed the positive effects of spinel phase on the mechanical properties of forsterite ceramic. It is shown that the formation of spinel phase strongly improved sinterability (relative density of 99%) and hardness (12.45 GPa) of forsterite bodies and the value of 3.2 MPa m$^{1/2}$ for indentation fracture toughness was reported [13]. Through this strategy Mg_2SiO_4-$MgAl_2O_4$ eutectic ceramics was also considered [14]. In the only preliminary found study, it is shown that directionally solidification allowed fabricating fine-microstructured Mg_2SiO_4-$MgAl_2O_4$ eutectic ceramics. However, no data of any property was reported in this study [14].

Concerning little works have done with Mg_2SiO_4-$MgAl_2O_4$ eutectic ceramics, so this study aims at preparation and investigation of improved ceramic composites based on Mg_2SiO_4-$MgAl_2O_4$ eutectic composition with variable growth rates and evaluate the possible beneficial effect of different growth velocities on their microstructure as well as

B.M. Moshtaghioun, et al.

their mechanical properties.

2. Experimental procedure

The starting materials were commercially available Al_2O_3 powder (Sigma-Aldrich, 99.99%), MgO powder (Sigma-Aldrich, > 99%) and SiO_2 (Mateck GmbH, 99.99%). MgO powder was dried in a furnace at 1200 °C for 12 h to remove the possible moisture absorption from outside air [15]. The eutectic point of Mg_2SiO_4 and $MgAl_2O_4$ appears at 71 wt% Mg_2SiO_4 and 29 wt% $MgAl_2O_4$ and its melting temperature is around 1720 °C that can be obtained by mixture of 48.79 wt% of MgO, 30.08 wt% of SiO_2 and 21.13 wt% of Al_2O_3 [14,16]. Precursor rods of ∼2.5 mm in diameter and up to ∼5 cm in length were prepared by cold isostatic pressing for 5 min at 200 MPa followed by pre-sintering in a furnace at 1300 °C for 12 h. Furthermore, Mg_2SiO_4 and $MgAl_2O_4$ monolithic ceramics were prepared for comparison.

Growing the eutectic rods by directional solidification from the melt using the laser-heated floating zone (LFZ) method with a CO_2 laser [17] was chosen to fabricate all ceramics explained before. The pre-sintered rods were then grown by LFZ in N_2 with a slight overpressure of 0.1–0.25 bar with respect to ambient pressure, to avoid the appearance of gas inclusions in the solidified rod [18]. In all cases using three-growth steps of diameter reduction at growth rate of 300 mm/h following with the last growth step without diameter reduction and using a variable growth rate between 10 and 500 mm/h were performed to evaluate its effect on the densification, microstructure and mechanical properties of the resulting Mg_2SiO_4-$MgAl_2O_4$ eutectic ceramics. A nominal laser output power of 25 W has been used in the last step to maintain a constant feed and very small molten zone. Three first steps were performed in contra-rotation of the crystal and precursor with 50 rpm and the last one was without rotation and eutectic rods of ∼1 mm in diameter and up to ∼20−30 cm in length were fabricated. Regarding Mg_2SiO_4 and $MgAl_2O_4$ monolithic ceramics, they were fabricated by the LFZ method, too. Later cases were grown using only one-growth step of mild diameter reduction at growth rate of 250 mm/h to eliminate porosity and they were grown later with the growth rate of 50 mm/h.

The transverse cross-sections of the grown eutectic rods were first cut, ground and polished to a 0.25 μm finish. Additionally, all were characterized microstructurally by a field emission scanning microscopy (FE-SEM) (model Merlin, Carl Zeiss, Germany) with an EDS microanalysis system INCA350 from Oxford Instruments. Microstructure observations were done from transverse sections using the back-scattered emission (BE) mode on carbon coated-polished surfaces.

Finally, mechanical properties were studied by Vickers-indentation tests (Matsuzawa MXT70 micro-hardness tester) applying a load of 4.9 N for 15 s on cross-sections of eutectic rods to evaluate Vickers hardness and indentation fracture toughness with at least fifteen tests [19,20]. The micro-hardness of Mg_2SiO_4 and $MgAl_2O_4$ monolithic ceramics were also measured by applying a load of 4.9 N. Nanoindentation tests (Agilent Technologies G200, U.S.A. equipped with a Berkovich indentor with a tip radius of 120 nm) at 250 mN with constant loading rate of 0.5 mN/s were done as well, to measure hardness and elastic modulus from loading-unloading curves. At least 50 acceptable tests were performed for each sample and the statistically analysis and considering the average makes us sure that measured hardness and elastic modulus values are correct. The flexural strength of the rods of 1 mm in diameter in longitudinal direction was measured by flexural tests carried out in a three-point bending test fixture of 10 mm loading span in Instron testing machine (Instron 5565). At least ten tests were performed at constant crossheads speed of 0.05 mm/min.

3. Results and discussion

Fig. 1 compares representative transverse cross section images of the Mg_2SiO_4-$MgAl_2O_4$ eutectic ceramics grown at different velocities

without rotation. In Table 1 the microstructural properties obtained from the analysis of the SEM images are summarized. By EDS analysis, the grey matrix was detected to be forsterite and light grey embedded phases were spinel. The microstructural characteristics from analysis de SEM images are listed in Table 1.

The presence of the porosity was an undesired feature for those grown at a growth rate lower than 50 mm/h. Furthermore, at the lowest growth rates of 10 mm/h, the relative density was ∼92% with the highest percentage of porosity (Fig. 1 A) and a well-aligned eutectic structure, the usual one, could not be observed (Fig. 1(A), inset). The reason why the most usual eutectic structure was rarely obtained in this system at the slowest growth rates is unknown. This result was reported before in literature [14]. When increasing the velocity to 25 mm/h, the microstructure approached to regular and homogeneous $MgAl_2O_4$ broken lamella phase in a continuous Mg_2SiO_4 matrix with a lower percentage of porosity and relative density of ∼98% (Fig. 1(B)). The relative orientation of the two phases must be < 100 > because this one minimises the elastic energy induced by the lattice misfit. This statement was reported elsewhere [14]. The perimeter of the $MgAl_2O_4$ phase was estimated as 2 × (width + length) and more than 100 lamellae were considered in all cases. This parameter was around 10.4 μm, for Mg_2SiO_4-$MgAl_2O_4$ eutectic ceramics grown at 25 mm/h. At 50 mm/h growth rate, the microstructure was totally consisted of finer lamellae randomly distributed in the matrix while pores were rarely seen, and relative density is about 100% (Fig. 1(C)). At this velocity, Mg_2AlO_4 lamellae with perimeters of 7.6 μm (Fig. 1(C), were distinguished. At higher velocities, such as 300 or 500 mm/h, a cell structure was completely dominant with a diameter of cell about 46 and 26 μm, respectively (Figs. 1(D) and (E)). Lamellar pattern within the cells with perimeter of 20.8 μm and 8.8 μm were estimated for velocities of 300 and 500 mm/h, respectively. In both velocities, some tiny pores were observed in cell boundaries and relative density is very close to the theoretical one. A new grey phase at the cell boundaries that EDS microanalysis showed to be composed of mainly O, Ca and some trace of Al, Si and Mg elements were found, too. This one seems to be a consequence of the segregation of impurities towards the melt upon solidification from the starting powders.

As it is well known, the eutectic system fulfills the Hunt–Jackson condition and the interspacing (λ) depends on the growth rate (*V*) according to the typical quadratic law of $\lambda = cV^{-1/2}$ where c is one constant [21]. The evolution of λ as a function of the growth rate *V* is plotted in Fig. 2. As expected, the higher the growth rate the smaller the interspacing, and the interspacing distance decreased to values as low as 500 nm for growth rates of 500 mm/h. The value of c that is obtained from Fig. 2, is equal to 5.14 $\mu m^{3/2}$ $s^{-1/2}$.

Micro-hardness and indentation fracture toughness of the eutectic rods and Mg_2SiO_4 and $MgAl_2O_4$ monolithic ceramics were determined from Vickers micro-hardness tests. Table 1 lists the average micro-hardness measured on the transverse cross-section of Mg_2SiO_4-$MgAl_2O_4$ eutectic rods grown at different velocities. They were within the range 11.0–13.5 GPa, except the one grown at 10 mm/h that showed a much lower average value of hardness (8 GPa) because of the large presence of porosity in the microstructure and much lower relative density. Furthermore, the ordered eutectic microstructure that can harden matrix in more efficient way was not observed at this velocity. Comparing with the value of hardness for Mg_2SiO_4 monolithic ceramics as a matrix (7.5 GPa), significant improvement of hardness was obtained through Mg_2SiO_4-$MgAl_2O_4$ eutectic ceramics, particularly the one grown at 50 mm/h (13.4 GPa) and it approached to the value of hardness for the $MgAl_2O_4$ monolithic ceramic (16.7 GPa). There is no clear dependence of hardness values with the interspacing, contrary to the common behavior of the improved hardness with the smaller interspacing (higher velocities) in fibrous eutectic ceramics [17]. The important microstructural feature controlling hardness is a lamella characteristic length associated to the size. We will adopt the perimeter since the smaller $MgAl_2O_4$ lamella perimeter, the more efficient for Mg_2SiO_4 matrix
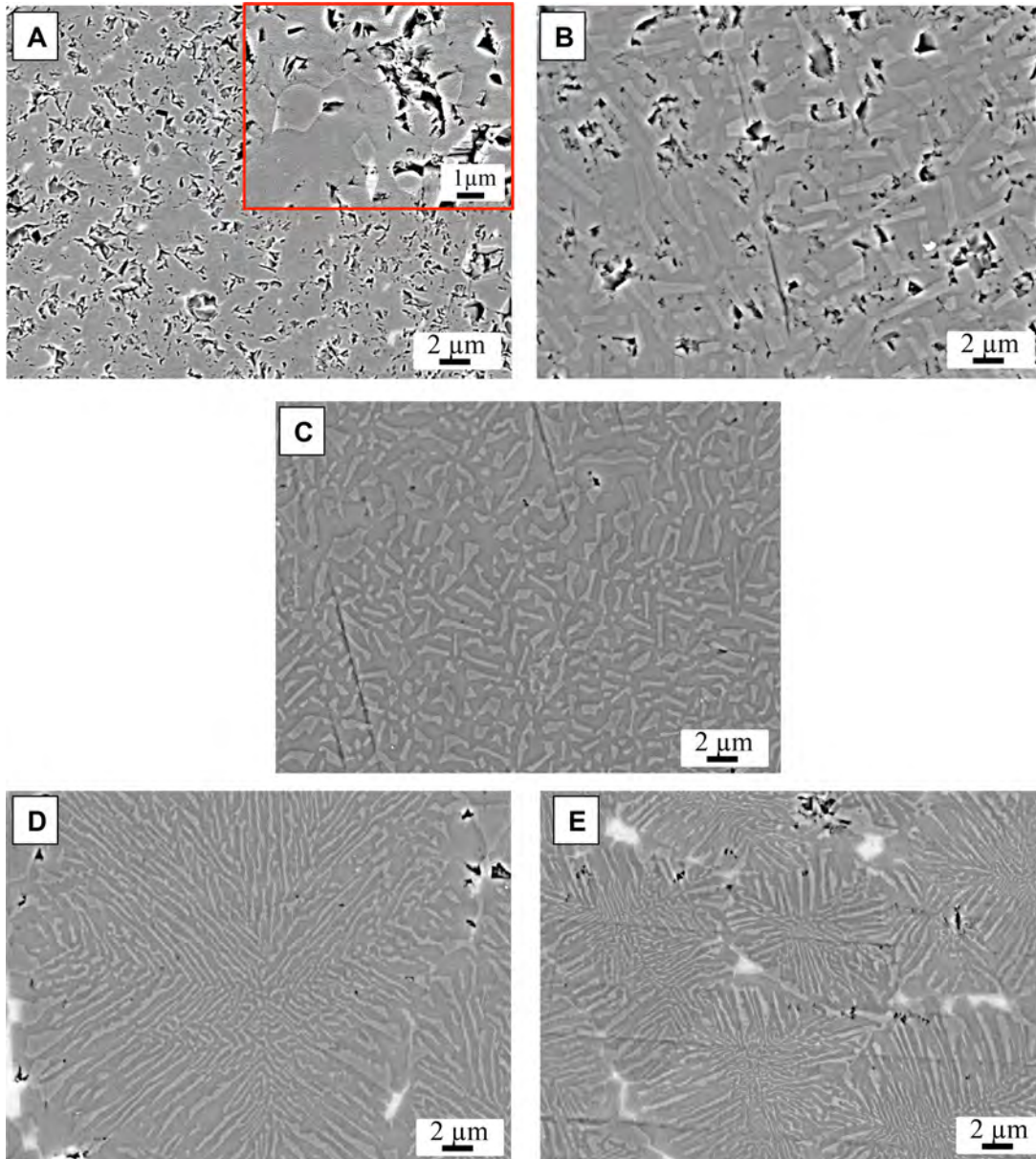
Fig. 1. Representative FE-SEM micrographs of Mg_2SiO_4-$MgAl_2O_4$ eutectic ceramic in transverse section by LFZ grown at (A) 10, (B) 25, (C) 50, (D) 300 and (E) 500 mm/h. For image (A), the inset shows higher magnification to see $MgAl_2O_4$ phase distribution.

hardening (Table 1).

This result can be rationalized by means of a classical model based upon the elastic theory of dislocations which has also been used for the interaction with small cracks and planar structures [22]. Certainly, the lamella array cannot be regarded as a dislocation array at all. However, the long-range stress field in the vicinity of one lamella can be modelled as the field created by a continuous density of screw dislocations. The screw character is required to ensure the rotation symmetry along the longer axis of one lamella. This modelling procedure has been extensively used in literature for other mesoscopic microstructures, such as small cracks commented above. The lamellar structure gives rise to an internal stress which can be calculated as follows: let us model the lamella as an array of continuous parallel straight screw dislocations aligned along the lamella axis. The total number of screw dislocations is represented by n. The thickness of the array is stood by $2l$. It is important to emphasize that this distance is the effective thickness of the array which would provide the same stress as the real lamella, but it not the real thickness of that one. Any dislocation intending to overcome

one lamella must surround it and bow a typical length $x \cong p/2\pi$, with p being the lamella perimeter. Assuming a constant dislocation density equal to $\rho = n/2l$ the stress in excess that one dislocation must overcome to surround a lamella would be given by:

$$\frac{1}{2\pi}\int_{-l}^{l}\frac{\mu b\rho}{x-y}dy = \frac{\mu b\rho}{2\pi}\ln\left(\frac{x+l}{x-l}\right) = \frac{\mu b\rho}{2\pi}\ln\left(1+\frac{2l}{x-l}\right)$$
$$= \frac{\mu b\rho}{2\pi}\ln\left(1+\frac{4\pi l}{p-2\pi l}\right) \quad (1)$$

Where μ is the shear modulus of $MgAl_2O_4$ (approximately equal to 109 GPa) [23], b the burgers vector of the dislocations in this material, $b\cong5.6$ Å, with a lattice parameter in a cubic structure $a\cong8$ Å [24], the contribution of the dislocations to hardness (H) is given by:

$$H = H_0 + \frac{\mu bn}{4\pi l}\ln\left(1+\frac{4\pi l}{p-2\pi l}\right) \quad (2)$$

Where H_0 is the intrinsic hardness of the matrix (i.e. hardness without

3

B.M. Moshtaghioun, et al.

Table 1
Average transverse microstructural features and mechanical response by Vickers indentation, nanoindentation and three-point bending tests in Mg$_2$SiO$_4$-MgAl$_2$O$_4$ eutectic ceramics grown at various rates by LFZ method.

| Material	Growth rate (mm/h)	Interspacing (μm)	Microstructural feature size					Relative density (%)	Vickers indentation for transversal sec. with load of 4.9 N			Nanoindentation for transversal sec. with load of 250 mN (GPa)		Flexural strength (σ$_f$) (MPa)
			Lamella (μm)		Cell (μm)				Hardness (HV0.5)	Hardness (GPa)	Toughness (MPa m$^{1/2}$)	Hardness	Elastic modulus	
			Length	2×(width + length)	Individual cell size	Interacell (lamella structure)								
						Length	2×(width + length)							
Mg$_2$SiO$_4$-MgAl$_2$O$_4$	10	–	–	–	–	–	–	92.4%	–	8.0 ± 0.9	–	–	–	–
	25	2.1 ± 0.4	4.2 ± 1.3	10.4 ± 2.8	–	–	–	97.7%	–	11.2 ± 0.7	3.5 ± 0.3	12.0 ± 1	223 ± 13	–
	50	1.1 ± 0.2	3.1 ± 0.4	7.6 ± 2.8	–	–	–	100%	–	13.4 ± 0.5	3.5 ± 0.3	15.3 ± 1	240 ± 20	430 ± 90
	300	0.7 ± 0.2	–	–	45.7 ± 4.5	10.0 ± 2.3	20.8 ± 5.0	99.2%	–	10.9 ± 0.6	2.5 ± 0.3	11.5 ± 1	239 ± 25	–
	500	0.5 ± 0.2	–	–	25.6 ± 2.6	4.5 ± 0.9	8.8 ± 2.0	99.6%	–	11.6 ± 0.9	2.5 ± 0.5	12.6 ± 1	242 ± 16	240 ± 65
MgAl$_2$O$_4$	50	–	–	–	–	–	–	100	–	16.7 ± 0.8	1.7 ± 0.1	20.6 ± 0.5	309 ± 5	–
Mg$_2$SiO$_4$	50	–	–	–	–	–	–	100	–	7.5 ± 1	2.5 ± 0.3	10.4 ± 2	197 ± 39	–
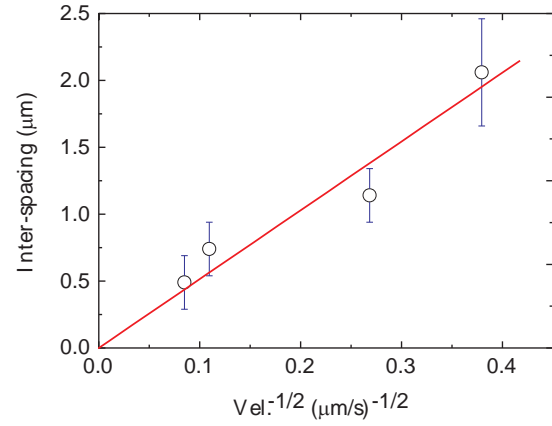
Fig. 2. Inter-spacing versus inverse square root of growth rate for Mg$_2$SiO$_4$-MgAl$_2$O$_4$ eutectic ceramics.
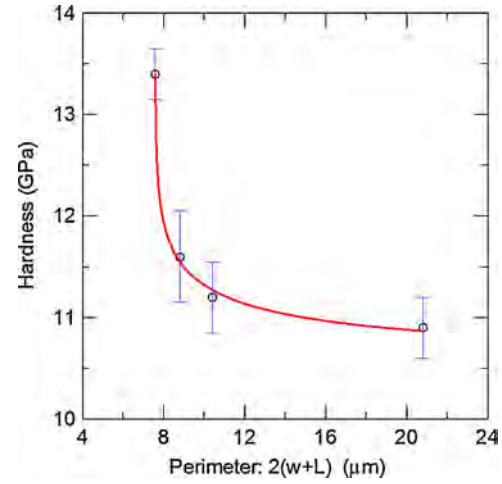

Fig. 3. Hardness versus dependence. The continuous line is the fitting to the theoretical prediction displayed in Eq. (2). Such fitting provides values for H$_0$≅10.6 GPa, n≅100 and 2πl≅7.53 μm. The regression factor is r≅0.998.

lamellae). The value of *n* can be obtained through a fitting of the experimental results to this law. This one is displayed in Fig. 3. The agreement is excellent, with a regression factor $r = 0.998$ and one value of 2l≅2.39 μm. Our fitting provides a value of n≅100. This value is consistent if we consider that the displacement induced by the full set of dislocations is of the order of nb≅560 nm. On the other hand, the number of unit cells (*N*) of MgAl$_2$O$_4$ along an array of length 2l is N≅2l/8≅3 × 10^3. Since *Mg$_2$SiO$_4$* has an orthorhombic structure with a'≅4.75 Å, b'≅10.20 Å and c'≅5.98 Å [25] the smallest misfit δ along the interface would be given for δ≅c' − a≅−2.02 Å. The accumulated mismatch along such array would be Nδ≅605 nm, which in the order of magnitude of the displacement calculated previously.

Fracture toughness was determined from the length of the cracks caused from the Vickers indentations. Although the indentation method is not considered appropriate for the absolute determination of fracture toughness [26] it is adequate to compare the values obtained from samples grown at different rates and to provide an estimation of the fracture toughness. Fig. 4(A) and (B) present well-defined cracks from indentation imprints for Mg$_2$SiO$_4$-MgAl$_2$O$_4$ eutectic ceramics grown at 50 mm/h and 500 mm/h, respectively. In the case of Mg$_2$SiO$_4$-MgAl$_2$O$_4$ eutectic ceramics grown at 50 mm/h, some evidence of weak interface between Mg$_2$SiO$_4$ and MgAl$_2$O$_4$ and crack deflection was observed (Fig. 4(C)) while crack propagation was trans-granular and the straight propagation of the crack through the eutectic structure was observed at grown rates as high as 500 mm/h (Fig. 4(D)). However, no important
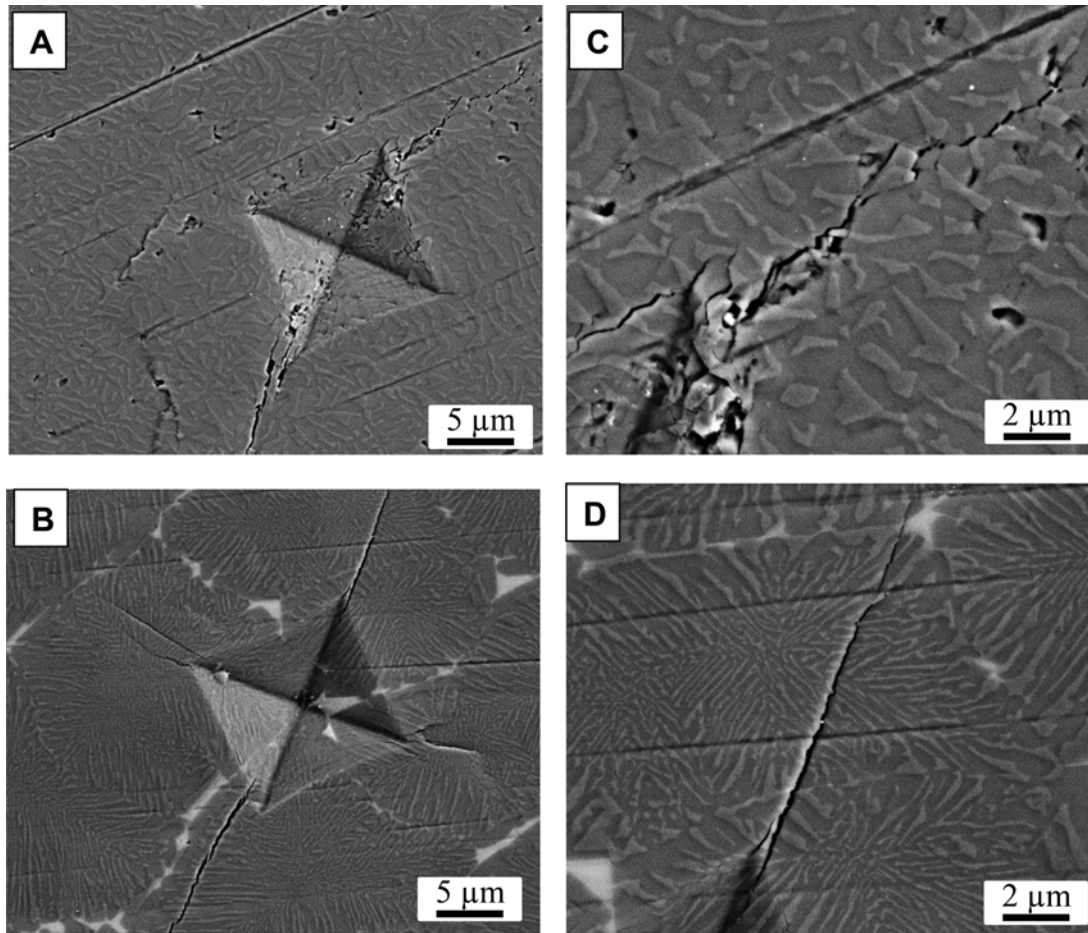
Fig. 4. (A-B) Cracking pattern and (C-D) crack propagation detail of the Mg_2SiO_4-$MgAl_2O_4$ eutectic ceramics grown at 50 and 500 mm/h under an indentation load of 4.9 N, respectively.

improvement was obtained in the mean value of indentation fracture toughness with either growth rate or lamella perimeter and all of them were around 2.5–3.5 MPa m$^{1/2}$(Table 1).

In order to reduce the influence of the microstructural defects like pores and micro-cracks inside the grown rod, hardness and elastic modulus were measured by nano-indentor for Mg_2SiO_4-$MgAl_2O_4$ eutectic ceramics grown at variable velocities and the values are listed in Table 1, too. Higher values of hardness by nano-indentor compared with Vickers from the same rods is a common fact reported before [27]. The same trend with lamella perimeter was observed and it reached to ~15 GPa for eutectic ceramics grown at 50 mm/h growth rate with the smallest lamella perimeter of 7.6 μm. Regarding elastic modulus, the value is ~220−240 GPa independent of solidification rate, although there is a narrow scatter. This behavior is expected because the volume fractions of the phases are the same for all growth rates and elastic modulus value is the representative of the both phases bonding magnitude. This value is comparable with elastic modulus calculated by the rule-of-mixture model (E Mg_2SiO_4 = 140−200 GPa [28], E $MgAl_2O_4$ = 290 GPa [29], therefore estimated E Mg_2SiO_4-$MgAl_2O_4$ eutectic (73:27 vol% $\cong$ 225 GPa).

Three-point bending tests were performed on eutectic ceramics grown at 50 and 500 mm/h at room temperature to study the evolution of the mechanical properties with microstructure. Table 1 lists the average bending strengths (σ_f) for these two velocities. The bending strength decreased as the growth rate increased from 430 MPa at 50 mm/h to 240 MPa at 500 mm/h. This former value was twice higher than that of 203 MPa previously reported in the literature for monolithic Mg_2SiO_4 [6] and it approached to the values reported for fine-

grained SPS´ed spinel [30].

Although higher interspacing was found for the one grown at 50 mm/h, higher values of σ_f can be correlated to the homogeneous dispersion of fine Mg_2AlO_4 lamellae in the Mg_2SiO_4 matrix. While for the one grown at 500 mm/h, weak inter-cells regions which probably contain pores and microcracks and more importantly larger lamellae act as the stress concentrators which nucleate the crack and resulted in lower value of strength. The fracture surface of the eutectic grown at 50 mm/h was rough at a microscopic level (Fig. 5A and 5A inset) and this may be due to the deflecting at interfaces or other defects. However, more flat fracture surface was observed for the Mg_2SiO_4-$MgAl_2O_4$ eutectic ceramic grown at 500 mm/h, indicating that the crack propagated along a straight path with less efficient deflecting at the interfaces (Fig. 5B and 5B inset).

4. Conclusions

Mg_2SiO_4-$MgAl_2O_4$ eutectic ceramics have been grown by laser-heated floating zone (LFZ) method. At lower growth rates of 25 and 50 mm/h, the microstructure was composed of lamellae of $MgAl_2O_4$ distributed on a dominant $MgSiO_4$ matrix with random orientation of those lamellae. Increasing growth rates to 300 mm/h and higher, the microstructure transformed and the cell structure was completely dominant with lamellar pattern within the cells. Hardness, fracture toughness and flexural strength have been studied. It was found that the highest hardness (13.4 GPa from Vickers indentation and 15.3 GPa from nanoindentation) and strength (~430 MPa) can be obtained for Mg_2SiO_4-$MgAl_2O_4$ eutectic ceramic grown at 50 mm/h growth rate

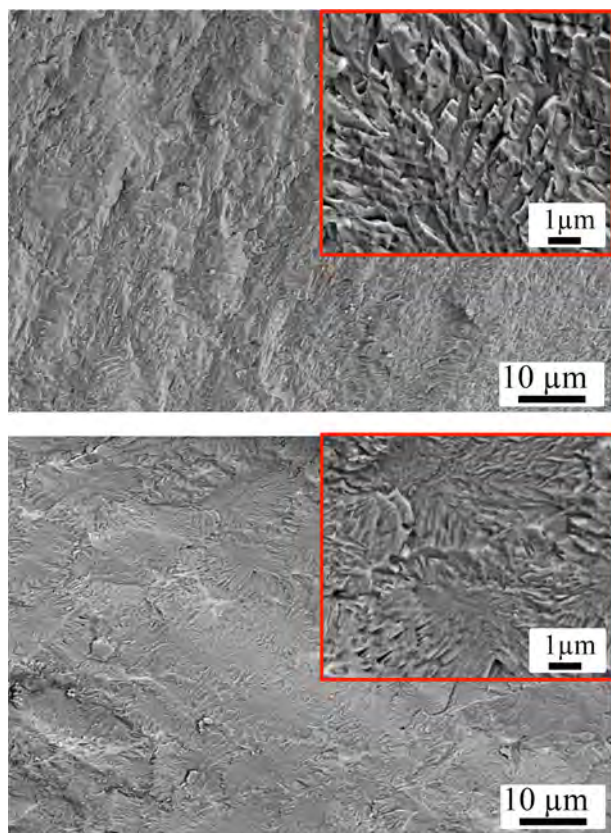**Fig. 5.** Fracture surfaces of Mg_2SiO_4-$MgAl_2O_4$ eutectic ceramics grown at (A) 50 mm/h and (B) 500 mm/h after bending testing at room temperature. For both images, the inset shows higher magnification to see more details in microscopic level.

with the smallest $MgAl_2O_4$ lamellae. As a remarkable achievement, it is reported that hardness depends on the average perimeter of lamellae. Such result has been explained in terms of a dislocation-based model based upon the residual stress induced by the presence of lamellae.

Declaration of Competing Interest

The authors declare that they have no known competing financial interests or personal relationships that could have appeared to influence the work reported in this paper.

Acknowledgements

References

[1] M. Kheradmandfard, S.F. Kashani-Bozorg, A.H. Noori-Alfesharaki, A. Zargar

Kharazi, M. Kheradmandfard, N. Abutalebi, Ultra-fast, highly efficient and green synthesis of bioactive forsterite nanopowder via microwave irradiation, Mater. Sci. Eng. C 92 (2018) 236–244.
[2] K.Y. Sara Lee, K.M. Christopher Chin, S. Ramesh, J. Purbolaksono, M.A. Hassan, M. Hamdi, W.D. Teng, Characterization of forsterite ceramics, J. Ceram. Process. Res. 14 (2013) 131–133.
[3] Y.C. Teh, C.Y. Tan, S. Ramesh, K.M. ChristopherChin, Y.M. Tan, B.K. Yap, M. Aimiriyan, The effect of sintering ramp rate on the sinterability of forsterite ceramics, Mater. Res. Innov. 18 (2014) S6-61-64.
[4] Y.M. Tan, Ch.Y. Tan, S. Ramesh, Y.Ch. Teh, Y.Ch. Ching, N. Lwin, B.K. Yap, D. Agrawal, Study on the effects of milling time and sintering temperature on the sinterability of forsterite (Mg2SiO4), J. Ceram. Soc. Japan. 123 (2015) 1032–1037.
[5] K.Y. Sara Lee, K.M. Christopher Chin, S. Ramesh, C.Y. Tan, W.D. Teng, I. Sopyan, Characterization of forsterite bioceramics, Adv. Mater. Res. 576 (2012) 195–198.
[6] S. Ni, L. Chou, J. Chang, Preparation and characterization of forsterite (Mg_2SiO_4) bioceramics, Ceram. Int. 33 (2007) 83–88.
[7] M.H. Fathi, M. Kharaziha, Two-step sintering of dense, nanostructural forsterite, Mater. Lett. 63 (2009) 1455–1458.
[8] M. Kharaziha, M.H. Fathi, Improvement of mechanical properties and biocompatibility of forsterite bioceramic addressed to bone tissue engineering materials, J. Mech. Behav. Biomed. 3 (2010) 530–537.
[9] S.A. Hassanzadeh-Tabrizi, Spark plasma sintering of forsterite nanopowder and mechanical properties of sintered materials, Ceram. Int. 43 (2017) 15714–15718.
[10] E. Mustafa, N. Khalil, A. Gamal, Sintering and microstructure of spinel–forsterite bodies, Ceram. Int. 28 (2002) 663–667.
[11] F. Tavangarian, R. Emadi, Synthesis and characterization of spinel–forsterite nanocomposites, Ceram. Int. 37 (2011) 2543–2548.
[12] R.M. Khattab, M.M.S. Wahsh, N.M. Khalil, Ceramic compositions based on nano forsterite/nano magnesium aluminate spinel powders, Mater. Chem. Phys. 166 (2015) 82–86.
[13] I.J. Shon, H.S. Kang, J.M. Doh, J.K. Yoon, Rapid Synthesis and Consolidation of Nanostructured Mg_2SiO_4-$MgAl_2O_4$ Composites, Mater. Trans. 52 (2011) 2007–2010.
[14] S. Kawakami, T. Yamada, S. Sakakibara, H. Tabata, Preparation of spinel fibers by directional solidification of $MgAl_2O_4$- Mg_2SiO_4 eutectic, J. Cryst. Growth 154 (1995) 193–196.
[15] C. Rode, T. Bunch-Nielsen, K.K. Hansen, B. Grelk, Moisture damage with magnesium oxide boards in Danish facade structures, Energy. Proc. 132 (2017) 765.
[16] L. Montanaro, Ch. Perrot, C. Esnouf, G. Thollet, G. Fantozzi, A. Negro, Sintering of industrial mullites in the presence of magnesia as a sintering aid, J. Am. Ceram. Soc. 83 (2000) 189–196.
[17] J. LLurca, V.M. Orera, Directionally solidified eutectic ceramic oxide, Prog. Mater. Sci. 51 (2006) 711.
[18] P.B. Oliete, J.I. Peña, Study of the gas inclusions in $Al_2O_3/Y_3Al_5O_{12}$ and $Al_2O_3/Y_3A_{15}O_{12}/ZrO_2$ eutectic fibers grown by laser floating zone, J. Cryst. Growth 304 (2007) 514–519.
[19] D.J. Green, An Introduction to the Mechanical Properties of Ceramics, Cambridge University Press, Cambridge, UK, 1998.
[20] G.R. Anstis, P. Chantikul, D.B. Marshall, B.R. Lawn, A critical evaluation of indentation techniques for measuring fracture toughness: I direct crack measurements, J. Am. Ceram. Soc. 64 (1981) 533.
[21] K.A. Jackson, J.D. Hunt, Lamellar and rod eutectic growth, Trans. Metal. SOc. AIME. 236 (1966) 1129.
[22] S. Lee, A new analysis of elastic interaction between a surface crack and parallel screw dislocations, Eng. Fract. Mech. 22 (1985) 429–435.
[23] Y. Zou, S. Gréaux, T. Irifune, B. Li, Y. Higo, Unusual pressure effect on the shear modulus in $Mg Al_2O_4$ spinel, J. Phys. Chem. 117 (2013) 24518–24526.
[24] T.E. Mitchel, L. Hwang, A.H. Heuer, Deformation in spinel, J. Mater. Sci. 11 (1976) 264–272.
[25] C. Klein, C. Hurlbut Jr, Manual of Mineralogy, 20th ed., Wiley, 1985, pp. 373–375 ISBN 978-0-471-80580-80589.
[26] G.D. Quinn, R.C. Bradt, On the Vickers indentation fracture toughness test, J. Am. Ceram. Soc. 90 (2007) 673–680.
[27] B.M. Moshtaghioun, J.I. Peña, Non-Hall-Petch hardness dependence in ultrafine fibrous MgO-$MgAl_2O_4$ eutectic ceramics fabricated by the laser-heated floating zone (LFZ) method, J. Eur. Ceram. Soc. 39 (2019) 3208.
[28] Ch.Sh. Zha, T.S. Duffy, R.T. Downs, H.K. Mao, R.J. Hemley, Sound velocity and elasticity of single-crystal forsterite to 16 GPa, J. Geophys. Res. 101 (1996) 17535–17545.
[29] A. Goldstein, A. Goldenberg, M. Vulfson, Development of a technology for the obtainment of fine grain size, transparent $MgAl_2O_4$ spinel parts, J. Ceram. Sci. Tech. 2 (2011) 1–8.
[30] M. Morita, B.N. Kim, K. Hiraga, H. Yoshida, Fabrication of transparent MgAl2O4 spinel polycrystal by spark plasma sintering processing, Scripta. Mater. 58 (2008) 1114–1117.